EUROPEAN MECHANICAL SCIENCE
e-ISSN: 2587-1110

Research Paper

Crack Analysis in the Sae 1117 Steel Shafts for Inclusion and Heat Treatment Combination Effect

Tuğrul Soyusinmez[1*], Murat Ardan Kayaaltı[2], Oğuzcan Güzelipek[3], Gökçe Akkuş[4], Taner Kavas[5]

[1,2,3,4]Totomak Machinery and Spare Parts Co., Turkey
[5]Afyon Kocatepe University; tkavas@aku.edu.tr
ORCID: T.Soyusinmez (0000-0001-8333-1961)

Abstract

Surface hardening in steels is a process in which a chemical composition is changed by thermo-chemical processes in a determined region and, accordingly, some micro-structure is changed. In order to obtain a harder layer than the inner region starting from the surface to a certain depth, it is mostly provided by diffusion of elements such as nitrogen and carbon. The process is particularly important in low and medium carbon steels in terms of increasing wear resistance, tensile strength and fatigue strength. The amount of elements used in cementation together with the duration of cementation is extremely important in terms of the harmonious change of structural differentiation. The effect of size and position of inclusions on the cracked structures which is affected from heat treatment is presented in the paper.

Keywords: Inclusion, Cracks, SAE 1117, Heat Treatment

1. INTRODUCTION

The surface hardening processes in the steels are the processes in which the chemical composition and thus some microstructure are changed by thermochemical processes in a determined region. In order to obtain a harder layer from the interior to a certain depth starting from the surface, it is mostly provided by the diffusion of elements such as nitrogen and carbon. The process is particularly important for low and medium carbon steels to improve wear resistance, tensile strength and fatigue strength. In addition, the amount of the element used in cementation and the time of cementation are extremely important for the change of structural differentiation.

On the other hand, it is also a fact that inclusions are formed due to different reasons during production / casting. The reasons for the inclusion are cast sand, pollution or slag mixing from the refractories are shown as the main reasons, but elemental (especially silica, alumina, manganese or iron oxide) impurities have been shown to cause differentiation in the melt.

We can define inclusions as foreign substances found in steels in general. These substances are generally particulate structures that are insoluble from the material matrix such as sulfur, oxide, silicate. One of the researchers, Sims, divides inclusions into two classes, which are endogenous and exogenous inclusions, respectively. The inclusion type as a result of the reactions in the molten metal is endogenous and its shapes, sizes and contents vary according to the process applied to the molten metal. Another type of inclusion, exogenous inclusions, is formed by the effect of slag formed during the production of steel. This inclusion was found to be larger, more irregular and complex in shape than endogenous inclusion [1,2]. In general, the size of the inclusions is greater than ~ 0.5 μm and is found as a chemical compound in the structure of metals and alloys. For example, the oxide (Al2O3) or sulphide (MnS) inclusions we see in the steel are the best examples. Many factors are caused by inclusion and we can list these factors as casting sand, pollution from the refractories or slag mixing. In addition to these main causes, elemental impurities also show differences in some regions. The inclusions are beneficial to the material rather than the harmful aspects. For example, oxide inclusions in the steel interact with dislocations to increase the hardness of the material and significantly change the yield strength of the material. One of the other positive factors provided by the inclusions is that they can be encountered in the automaton steels with resulfillations. Thanks to the resulphurisation, MnS inclusions in the steel are formed and the workability of the material is increased. In addition to this, increasing

*Corresponding authour
Email: tsoyusinmez@totomak.com.tr

European Mechanical Science, December 2018; 2(4): 119-127
doi: https://doi.org/10.26701/ems.477224
Received: November 6, 2018
Accepted: November 20, 2018

MnS sizes and decreasing MnS amount increase the workability [3]. As it is understood from the examples given, inclusions can be harmful or useful, and the general factors that determine this are the types, sizes, shapes, distributions and quantities. The inclusions are usually multi-phase and the composition of inclusions in the steel varies according to the elemental content of the steel. Polarized light and electron-probe micro analyzer are used to determine inclusions. In this article, inclusions occurring in steel shafts were examined with microscopic camera systems and the cracks produced by inclusions were analyzed.

2. METHODOLOGY

In this study, microstructure and inclusion studies were planned on the samples (Figure 1. a) and the samples were first cut by water jet so that the microstructure was not affected from the external conditions as shown in Figure 1. b.

Then, the samples were re-cut with the help of water jet and the surface was polished for microstructure studies. Representative samples obtained after first cutting with water jet has been shown in Figure 2. Parts are polished after being cut with water jet. Figure 3 shows the dimensioning of the samples after the second cut (a), unpolished parts (b), and photos after polishing (c). The images of this experiment, which are examined by camera system. As experimental method, two types of methods can be used for inclusions. The first of these is microscopic test methods and the polished surface is examined by a light microscope and several representative photographs are made by reporting the inclusion types encountered in the sample. Surface polishing is carried out for a satisfactory and more consistent result. The experiment is carried out with samples from three different positions of the part. In order to determine the microscopic image, the polished surface area should be minimum 160 mm^2. In addition, the section taken from the sample should be parallel to the longitudinal plane and perpendicular to the rolling plane of the section.

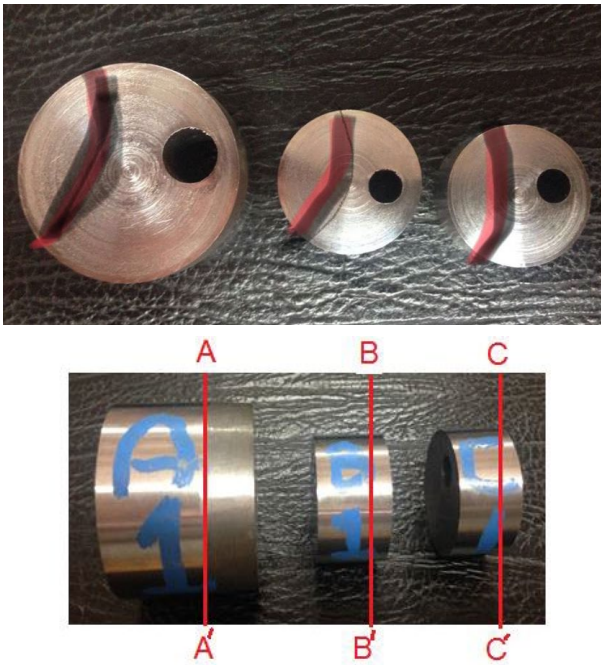

Figure 1. a) Representative examples provided by the Totomak A.Ş. b) First Water jet cutting of samples

Figure 2. a) Representative samples obtained after first cutting with water jet b) Second cutting lines of samples

Figure 3. a) Dimensioning of the samples after the second cut. b) Unpolished parts, c) Polished parts

Each sample was first examined by polarizing microscope and the images of each group are given below.

For the group A;
Figure 4 shows the image taken at 20 magnifications from sample A1. Figure 5 shows the image taken at 20 magnifications from sample A2. Figure 6 shows the image taken at 20 magnifications from sample A3.

For the group B;
Figure 7 shows the image taken at 20 magnifications from sample B1. Figure 8 shows the image taken at 20 magnifications from sample B2. Figure 9 shows the image taken at 20 magnifications from sample B3.

For the group C;
Figure 10 shows the image taken at 20 magnifications from sample C1. Figure 11 shows the image taken at 20 magnifications from sample C2. Figure 12 shows the image taken at 20 magnifications from sample C3.

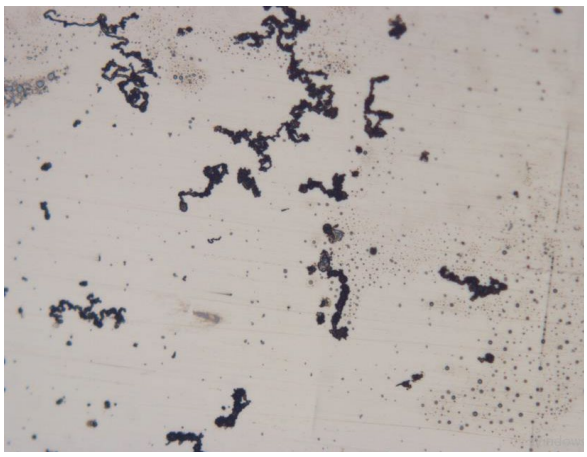

Figure 4. Sample A1 (20X)

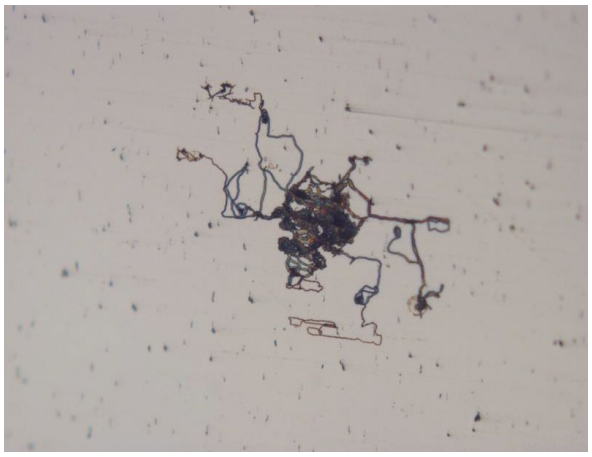

Figure 5. Sample A2 (20X)

Figure 6. Sample A3 (20X)

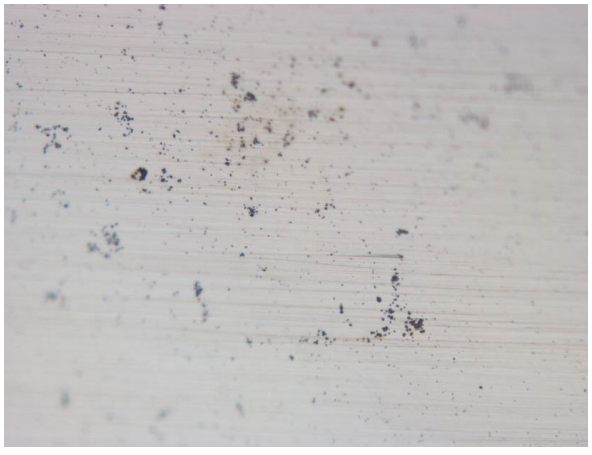

Figure 7. Sample B1 (20X)

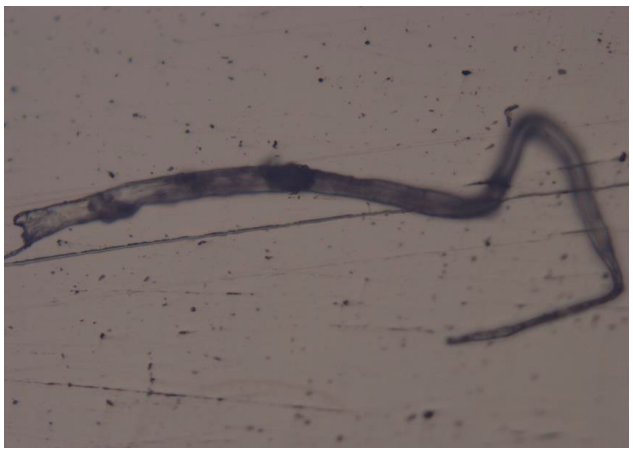

Figure 8. Sample B2 (20X)

Figure 9. Sample B3 (20X)

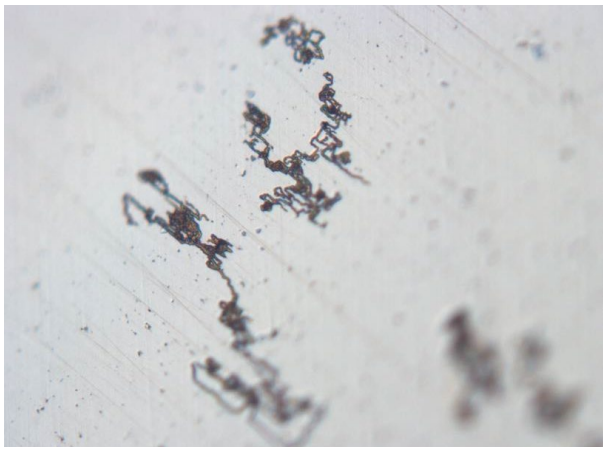

Figure 10. Sample C1 (20X)

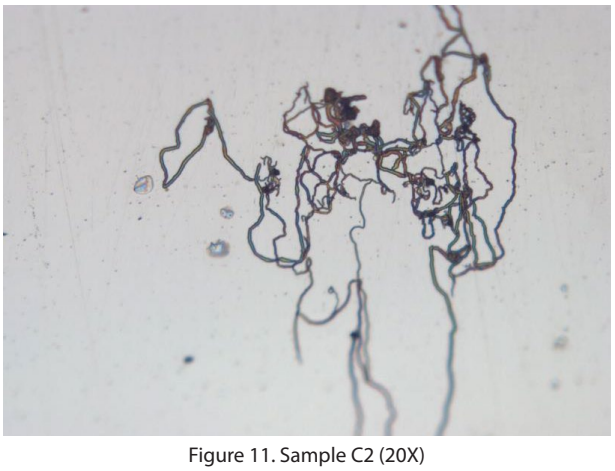

Figure 11. Sample C2 (20X)

Figure 12. Sample C3 (20X)

On the other hand, the samples with the most intense inclusion and superficial cavities under polarizing microscope were firstly taken before the polishing and then after the polishing (SEM) images and the figures obtained are given below. In addition, chemical analysis and elemental mapping analysis were performed for each group.

For the group A;

Figure 13 shows the elemental mapping of A group sample. As shown in figure 13, the red colors show the iron element, the green colors are carbon and blue colors are aluminum. The microstructure area of the elemental mapping analysis is shown in Figure 14. In addition, chemical analysis was performed on the yellow line determined in Figure 14. The results of the chemical analysis are shows in Figure 14.

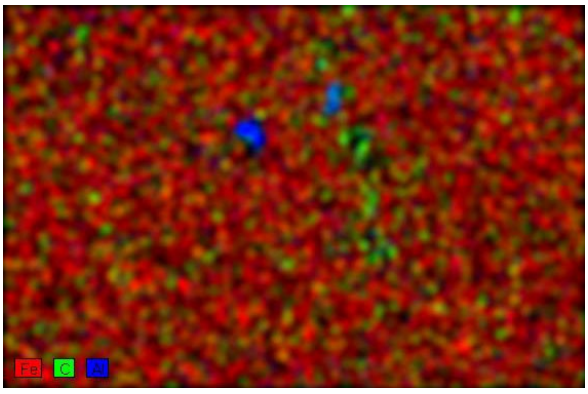

Figure 13. Elemental mapping of A coded sample

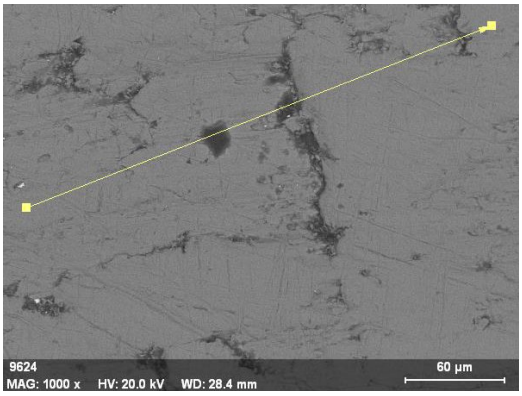

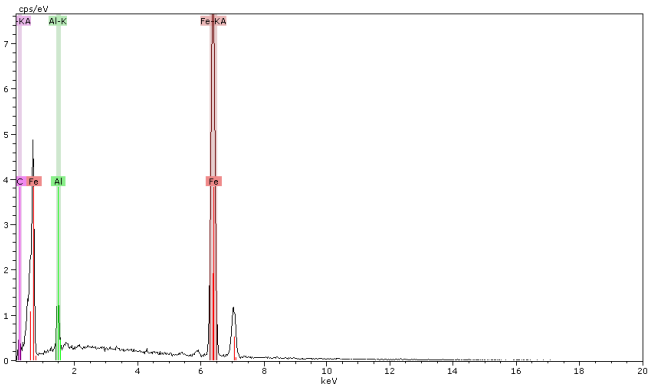

Figure 14. Chemical analysis of group A along the axis

For the group B;

Figure 15 shows the elemental mapping of B group sample. As shown in figure 15, the red colors show the iron element, the green colors are carbon and blue colors are aluminum. The microstructure area of the elemental mapping analysis is shown in Figure 16. In addition, chemical analysis was performed on the green line area in Figure 16. The results of the chemical analysis are shows in Figure 16.

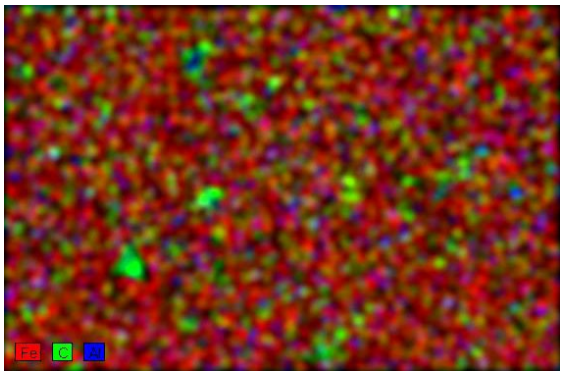

Figure 15. Elemental mapping of B coded sample

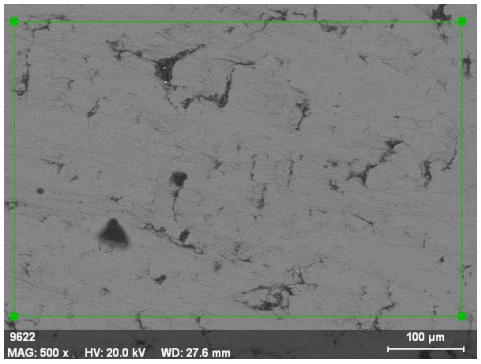

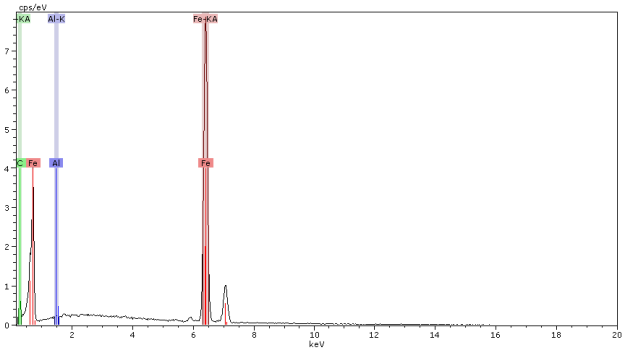

Figure 16. Chemical analysis of group B along the axis

doi: https://doi.org/10.26701/ems.477224

For the group C;

Figure 17 shows the elemental mapping of C group sample. As shown in figure 17, the red colors show the iron element, the green colors are carbon and blue colors are aluminum. The microstructure area of the elemental mapping analysis is shown in Figure 18. In addition, chemical analysis was performed on the green line area in Figure 18. The results of the chemical analysis are shows in Figure 18.

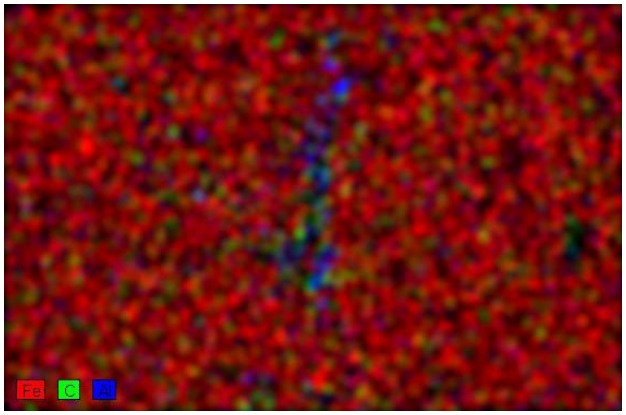

Figure 17. Elemental mapping and chemical analysis of C coded sample

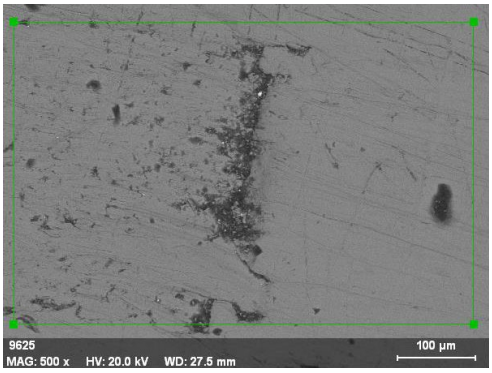

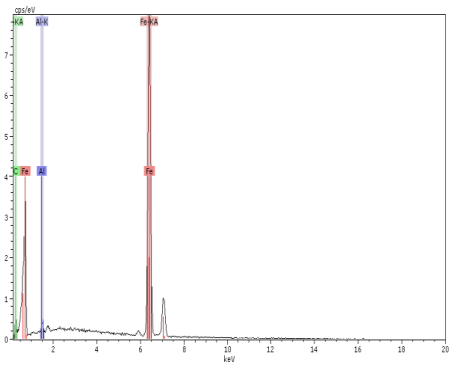

Figure 18. Chemical analysis of group C along the axis

Following the microstructure analysis above, section analyzes of each sample were carried out and the data obtained are given below.

Figure 19 show the vertical section microstructure image and chemical analysis of sample A. Figure 20 show the vertical section microstructure image and chemical analysis of sample B. Figure 21 show the vertical section microstructure image and chemical analysis of sample C.

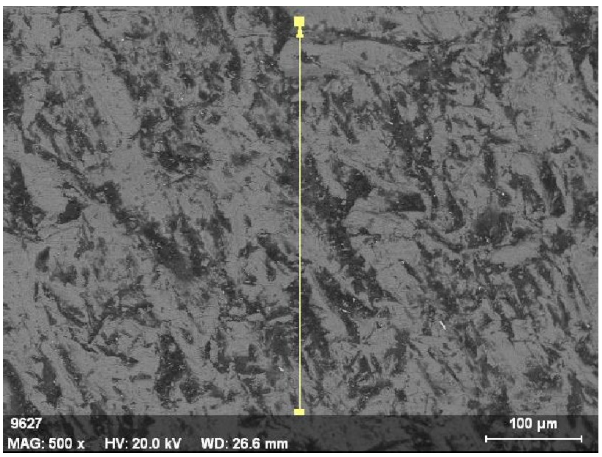

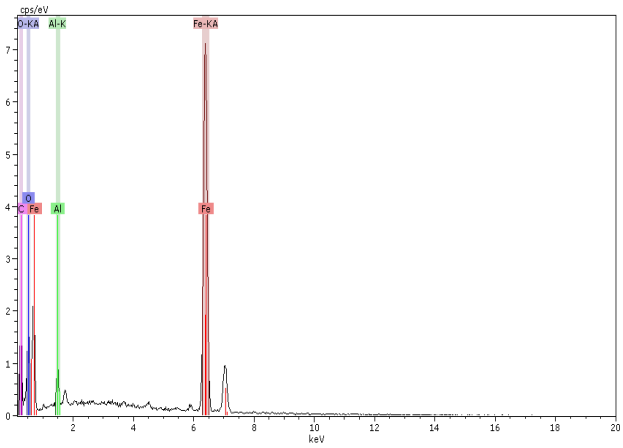

Figure 19. Vertical section microstructure image and chemical analysis of sample A

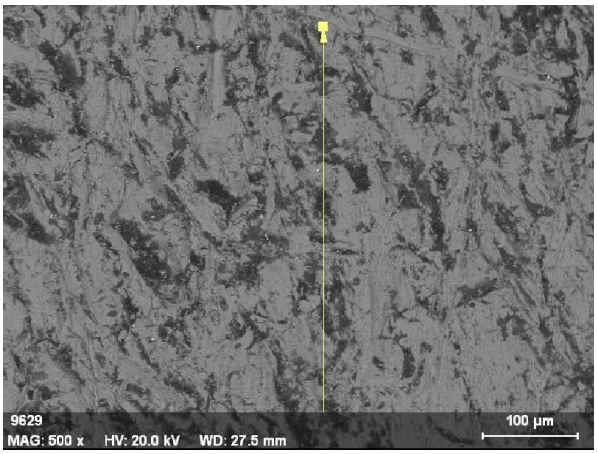

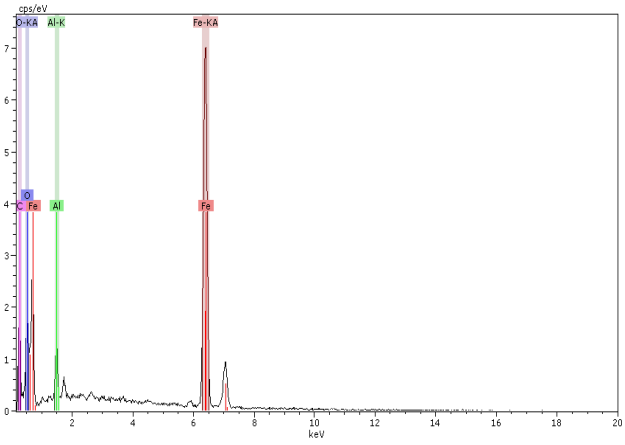

Figure 20. Vertical section microstructure image and chemical analysis of sample B

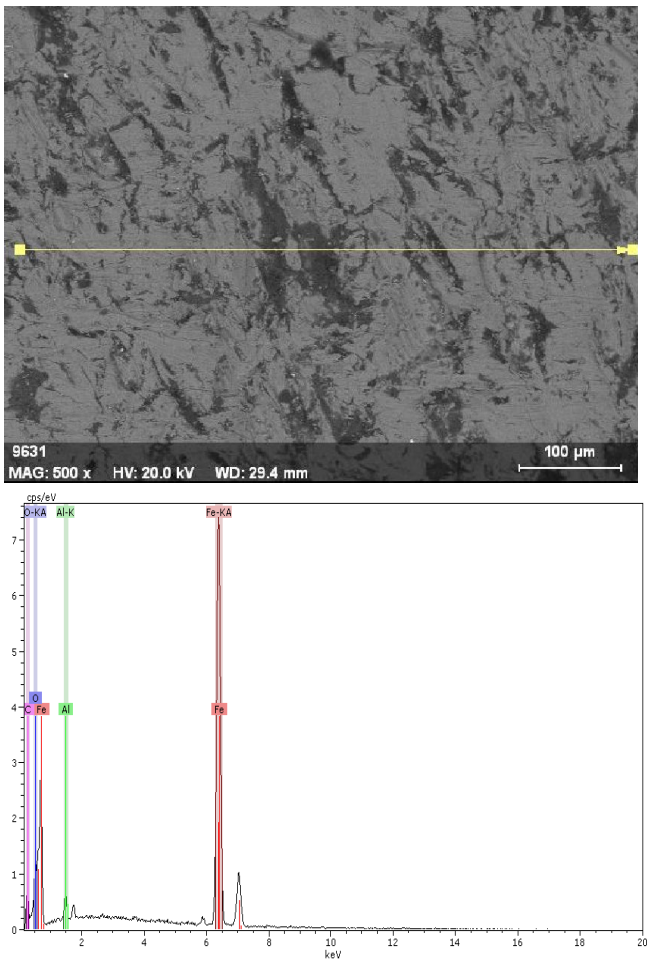

Figure 21. Vertical section microstructure image and chemical analysis of sample C

Finally, the surface of each sample was polished and then the electron microscope image was taken. Their microstructure images are given below.

Figure 22. show the polished surface microstructure analysis of sample A. Figure 23. show the polished surface microstructure analysis of sample B. Figure 24. show the polished surface microstructure analysis of sample C.

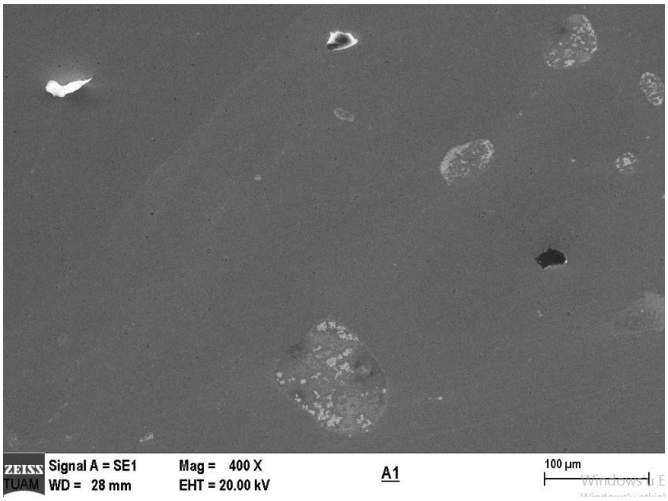

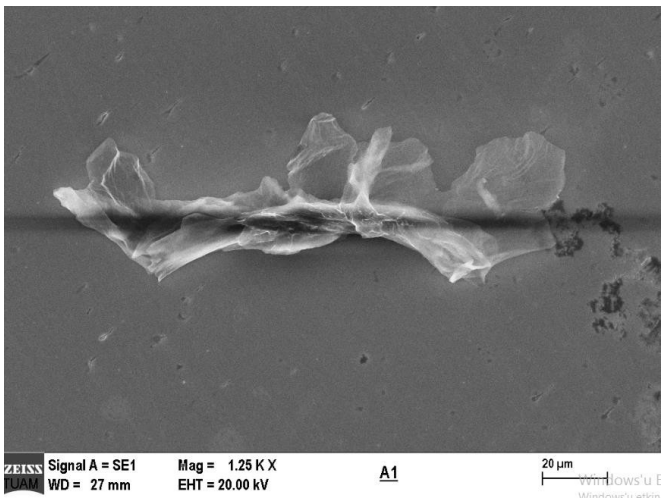

Figure 22. Polished surface microstructure analysis of sample A

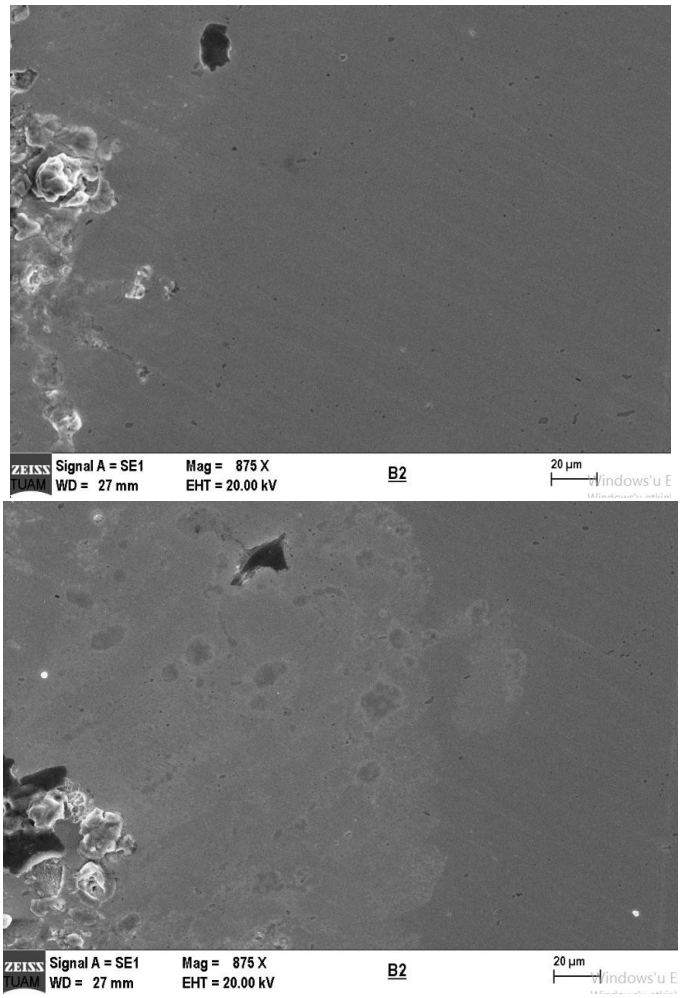

Figure 23. Polished surface microstructure analysis of sample B

doi: https://doi.org/10.26701/ems.477224

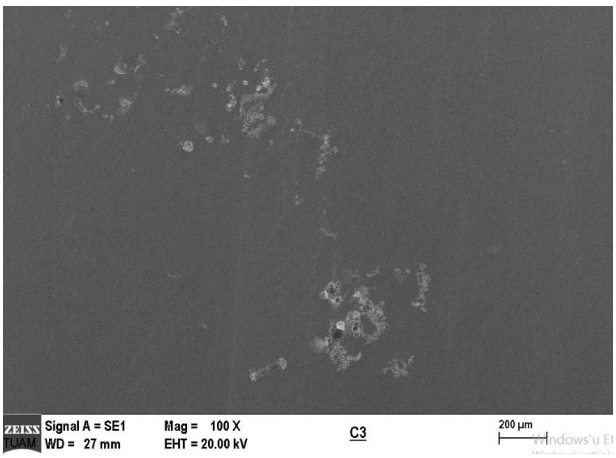

Figure 24. Polished surface microstructure analysis of sample C

3. RESULTS

As a result of the analyzes, all inclusions seen in the parts are solved as a result of optimization of heat treatment parameters as they are in ASTM E45 standards [4]. Trial parameters and results are shown on Table 1.

Table 1. Trial parameters and results

	Original Recipe	Trial 1	Trial 2	Trial 3	Trial 4
Preheating Temperature (°C)	420	420	420	420	450
Carburizing Temperature (°C)	960	960	960	960	960
Boost Cp (%)	1.35	1.35	1.35	1.20	1.20
Boost Time (min)	65	65	65	65	65
Difusion Cp (%)	1.00	0.80	1.00	0.80	1.00
Difusion Time (min)	20	20	20	35	45
Quenching Temperature (°C)	860	820	880	880	880
Soak Time At Quenching Temp. (min)	20	20	20	20	60
Oil Agitators Speed (rpm)	1400	800	1400	1400	1400

TRAIL 1

Purpose: Decreasing the stress of heat treatment step to material.

It's thought that if an amount of stress, which steel with high inclusions can stand, is loaded, there will be no cracks.

Action: Decreasing diffusion Cp to have low amount of martensite, decreasing quenching temperature to have less thermal shock, decreasing oil agitation to have slower cooling rate.

Conclusion: Good hardness values, there are still radial cracks. It is approved that crack is not related with stress which comes from heat treatment step. The cracks after the trail 1 is shown in the Figure 25.

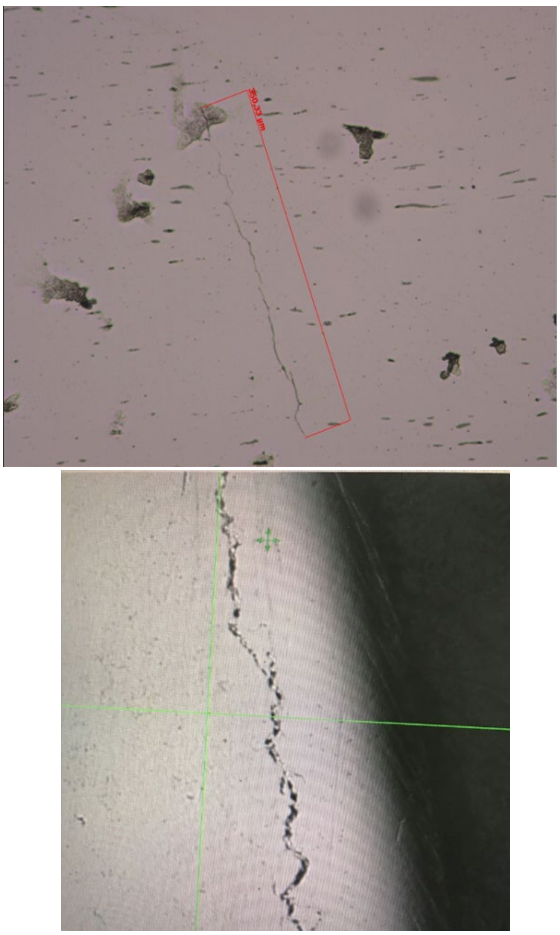

Figure 25. Results of Trial 1

TRAIL 2

Purpose: Decreasing the volume change difference between case and core.

It's thought that if the amount of martensite in the core is increased, there will be less stress gradians between case and core.

Action: Increasing quenching temperature.

Conclusion: Good hardness values, there is no radial cracks, but there are cracks which reach to surface (cylindrical area of pin). The volume change difference idea works. It is evaluated carbides which cause cracks at surface area. The cracks after the trail 2 is shown in the Figure 26.

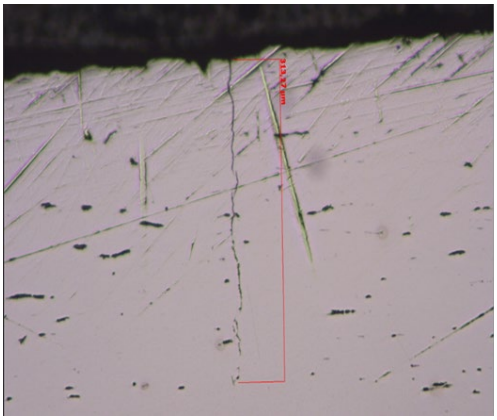

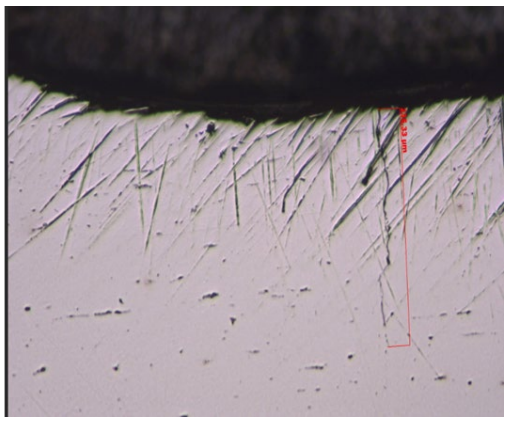

Figure 26. Results of Trial 2

TRAIL 3

Purpose: Getting rid of carbides which cause cracks on grain boundaries.

Action: Decreasing boost Cp, decreasing diffusion Cp, increasing diffusion time.

Conclusion: Good hardness values, there is no radial cracks, but there are still cracks which reach to surface (cylindrical area of pin). Retained austenite decreased below 3%, especially at crack area. It is observed less carbides. The cracks after the trail 3 is shown in the Figure 27.

Figure 27. Results of Trial 3

TRAIL 4

Purpose: Increasing retained austinite to have more elastic case structure, decreasing thermal shocks between preheating and carburizing process, to be sure all parts are at quenching temperature just before quenching step.

Action: Increasing diffusion Cp and time, increasing preheat temperature, decreasing furnace temperature at idle condition, increasing soak time at quenching temperature.

Conclusion: Good hardness values, we don't have any cracks. Retained austenite increased to 8%. The microstructure images observed after the trail 4 are shown in Figure 28.

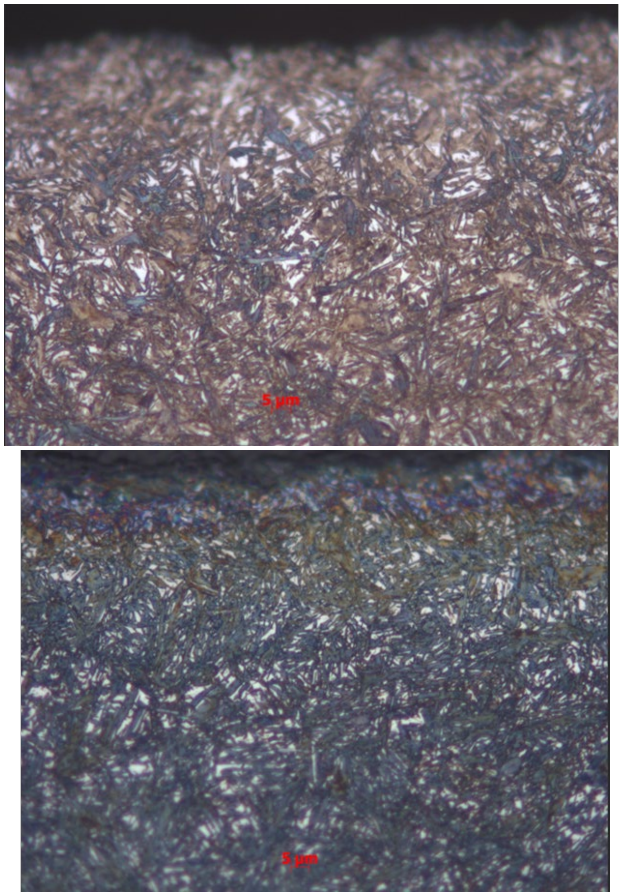

Figure 28. Results of Trial 4

4. CONCLUSION

The micro-structure and chemical analysis of the samples A, B and C and the water-jet specimens are given below.

- All 3 groups (A, B and C) were found to contain variable and similar proportions of superficial voids and inclusion in the sample.
- It is determined that the source of the cavities and inclusions formed in each of the 3 groups are mostly Al, Mn and Si-sourced.
- It is seen that B group samples contain more superficial space (spherical) than other samples.
- In each of the 3 groups, the gap and the inclusion were determined to be at the level of all the other steels and sometimes slightly more (especially at A and C).
- The inclusions and gaps determined in all three samples are thought to originate from the secondary elements entering the structure externally during the shaping of the metal.

- All samples had inclusions and gaps in a non-homogeneous structure. In addition, all 3 samples show a change in shape.
- Polarized microscopy studies in the samples showed fewer coarse grains. In the electron microscope examination, there was more space and inclusion (about 5-10 microns in size), which was small but did not affect the properties. Furthermore, it was observed that linear errors increased in A and C sample as the magnification increased. This is interpreted as the formation of linear grain boundaries during formation of nucleation due to conditions during cooling. Moreover, these linear structures are thought to occur due to different surface energies (properties or contact angles) of the secondary elements in the system.
- Both micro and macro segregation were observed in all samples.
- It is thought that the larger dimensional defects determined in the samples may be caused by the difference in dissolution during casting.

As a result; It is thought that the cavities and inclusions determined in all samples are at a level that will not significantly affect the mechanical or chemical wear, hardness, mechanical friction resistance, elastic modulus, ductility, fracture behaviour and load during operation. In addition, the non-cracking heat treatment parameter was determined from the result of 4 different heat treatment parameters. As a result, the heat treatment parameters have been optimized and the crack problem has been solved.

REFERENCES

[1] "Metallography and Microstructure", Metals Handbook, American Society for Metals, Vol. 9, p. 9, 1985.

[2] C. E. Sims, "Transactions of the Metallurgical Society of AIME", p. 367-393, 1959.

[3] R. Kiessling and N. Lange, "Non-Metallic Inclusions in Steel", Second Edition, Book No. 194, 1978.

[4] ASTM E45-18a, Standard Test Methods for Determining the Inclusion Content of Steel, ASTM International, West Conshohocken, PA, 2018, www.astm.org